



From resin formulation and process parameters to the final mechanical properties of 3D printed acrylate materials

Laura Schittecatte and Valérie Geertsen, Université Paris-Saclay, CEA, CNRS, NIMBE, LIONS, 91191 Gif-sur-Yvette, France

Daniel Bonamy, Université Paris-Saclay, CEA, CNRS, SPEC, 91191 Gif-sur-Yvette, France

Thuy Nguyen, Léonard de Vinci Pôle Universitaire, Research Center, 92916 Paris La Défense, France; Université Paris-Saclay, CEA, CNRS, SPEC, 91191 Gif-sur-Yvette, France

Patrick Guenoun , Université Paris-Saclay, CEA, CNRS, NIMBE, LIONS, 91191 Gif-sur-Yvette, France

Address all correspondence to Patrick Guenoun at patrick.guenoun@cea.fr

(Received 5 January 2023; accepted 23 February 2023; published online: 7 April 2023)

Abstract

Photopolymerizable resins are increasingly used to generate complex 3D printed parts through stereo lithography, digital light processing (DLP) and liquid crystal display (LCD) 3D printing. Many challenges relating to the resin chemistry and printing parameters still exist and must be addressed in order to entirely control the properties of parts after printing. This work reviews the current knowledge and describes the potential of DLP/LCD methods for printed acrylate resins, as well as the steps necessary to achieve a better control over the mechanical properties of printed materials.

Introduction

The development of additive manufacturing as we now know it has been a long process, its conceptualization dating back to the 1940s. It was in the 1970–1980s that the idea of spatially solidifying a polymer with light was first introduced: Dr. Hideo Kodama described a rapid prototyping technology based on a laser process in a patent that was abandoned after one year. In 1984, a trio of researchers from the French National Center for Scientific Research (CNRS) and the Cilas/Alcatel company filed another patent describing the layer-by-layer surface photopolymerization of an object also using a laser, and they printed a small staircase to prove the concept. Three weeks later, Chuck Hull filed a separate patent also to build small objects layer-by-layer but using UV light.^[1] The French patent was abandoned for a lack of industrial interest, whereas Chuck Hull developed the invention into a company and introduced the term “stereolithography” (SLA) in 1986.^[2,3] Digital light processing (DLP) technology^[4] was only introduced in the beginning of the 2000s, followed by liquid crystal display (LCD) printing.^[5]

Today, the layer-by-layer printing of objects with photopolymerization is dominated by these three technologies: SLA, DLP and LCD. Currently, SLA printing is more widely used in scientific fields and laboratories,^[6–9] whereas DLP and LCD printings are more common for home use.

All three technologies rely on the photopolymerization of a liquid resin at the bottom of a fluid reservoir. Most resins are composed, at least in part, of acrylate species, the polymerization of which is fast at ambient temperature. The formulation of these resins is crucial as it affects every step of the process from the printing parameters to the properties of the final object.

New printable polymer materials are emerging every year. They can be distinguished by their different properties: their

biocompatibility for bioengineering applications^[10–12] and dentistry,^[13–15] their optical properties,^[16] or their ability to respond to stimuli (4D printing).^[17,18] Additionally, these materials can present a range of mechanical properties. They can be either soft or stiff, which is of great interest, especially in the aerospace,^[8] energy, and construction industries.^[19,20]

Many publications are devoted to the relationship between the final mechanical properties of objects and their processing routes.^[12,21–28] However, between both the formulation of the resin and the printing process itself, many interconnected parameters must be taken into account. This review aims at establishing a consensus of the state-of-the-art from all these different studies, results and viewpoints. This will be achieved by analyzing the chemistry of acrylate resins, through methods such as fourier transformed infrared (FTIR), rheology, differential scanning calorimetry (DSC) or UV–visible spectroscopy. The resulting mechanical properties of printed parts will also be investigated through mechanical constants presented in Table I, all of which are defined in the hypothesis of isotropic materials and linear elastic fracture mechanics (brittle fracture).^[29]

Different types of 3D printers

As mentioned in the introduction, the 3D printing vat photopolymerization principle was introduced many years ago and has therefore been widely described in the literature.^[2,30] Today, three technologies for the 3D printing of photopolymerization resins—SLA, DLP and LCD—are mainly used, each differing by their illumination process.

SLA (for stereolithography) photopolymerization makes use of a laser with a given spatial resolution that locally polymerizes the

Table I. Table of the different mechanical constants of 3D printed materials analyzed in this review.

Constant	Name	Definition	Characterization Technique	
σ_y	Yield tensile strength	Maximal amount of stress a material can withstand before exhibiting a plastic deformation (unit: N/m^2). Constraint at which the material no longer deforms in an elastic manner, The stress writes $\sigma = F/A$ with F the force applied (N) and A the area of the loaded sample (m^2)	<p>Static tensile test scheme.^[29]</p>	
ϵ_y	Yield tensile strain	Relative elongation at the yield tensile stress (%), Elongation $\epsilon = \frac{l-l_0}{l_0}$, with l the length of the sample during the test and l_0 the initial length		
σ_{UTS}	Ultimate tensile strength	Maximal amount of stress a material can withstand before breaking (unit: N/m^2)		
ϵ_{UTS}	Ultimate tensile strain	Elongation at the ultimate tensile strength σ_{UTS} (%)		
σ_f	Breakage tensile strength	Tensile stress at material breakage (unit: N/m^2) ^a		
ϵ_f	Breakage tensile strain	Elongation at material breakage (%)		
E	Young's modulus	Characterizes the stiffness of a material submitted to a uniaxial stress in the linear elastic regime. Defined as the ratio of the stress (σ) to the strain (ϵ) in the linear tensile elastic domain (unit: Pa), e.g. via a static tensile test. ^[29]		
E' and E''	Storage and loss modulus	Dynamic determination at a given frequency is possible by Dynamic Mechanical Analysis (DMA) where the storage (E') and loss modulus (E'') are measured. They correspond respectively to the stored and dissipated energy for viscoelastic materials. ^{[29],b}		<p>DMA (Dynamic Mechanical Analysis) principle.^[29] Wedge spitting test, Compact Tension...</p>
K_{IC}	Toughness	Ability of a material to resist fracture propagation (unit: J/m^2)		Indentation hardness test, scratch test, Vickers Hardness test...
H	Hardness	Ability of a material to resist to permanent deformation, such as scratching, cutting, abrasion, indentation or penetration (unit: N/m^2)		

^aThe yield strength, ultimate tensile strength and breakage tensile strength are different for ductile materials (materials able to deform plastically). However, the acrylate resin polymers studied in this review are brittle materials, thus, the yield tensile strength and breakage tensile strength are equal in most cases.

^bSome articles make use of static tensile test experiments to determine Young's modulus, while others make use of dynamic mechanical analysis (DMA) to determine the so-called storage modulus.

resin [Fig. 1(a)]. The object is polymerized point-by-point along the laser path. This technique is repeatable and enables the printing of rather large objects, although it is very time consuming because it is a point-by-point process.^[31] An important parameter in SLA

printing is the hatching of the laser beam (distance between the center of two laser scans), which can limit the resolution.^[2,32]

DLP photopolymerization solves the problem of the slow point-by-point printing by projecting the laser as an entire 2D design onto a layer^[33,34] [Fig. 1(b)]. Here, the printing speed

can be as fast as 0.5 to 15 mm/s^[35] and with a resolution of about 100 μm.^[31,34] The main inconvenience of DLP is that only small objects can be printed (due to the reduction of the projector size to ensure high precision).^[2] Additionally, possible optical distortions due to the projector must be addressed.

In LCD printing, an LCD screen is placed directly under the resin vat [Fig. 1(c)], where direct contact of the screen on the vat avoids optical distortions. The printing is also layer-by-layer and the resolution depends on the screen pixel size, and normally a resolution of 50 to 150 μm can be reasonably expected with LCD technology.^[36,37] However, it is possible to go beyond this resolution with newer software developments. For example, LCD allows printing not only in black or white pixel, but also with different grey levels, enabling very high resolution (some publications claim a 10 μm in-plane resolution^[35]). Finally, the loss of light energy due to the absorption of the screen must be emphasized; approximately 90% of the light is absorbed by the LCD screen.^[31] Moreover, the direct contact of the screen with the vat bottom hinders control of the oxygen level at the polymerization site, which may cause many printing failures.

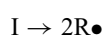
Although the same photochemical polymerization reaction occurs in all three of these techniques, the resin must be adapted for each process. Indeed, DLP and LCD resins are more reactive than SLA resins because the power density of the light used is inferior.^[34] Therefore, it is necessary to reformulate the resins to fit each process. To do so, in the next section, we describe the use of Jacobs' law as an efficient tool to compare resins reactivity.

The photopolymerization reaction

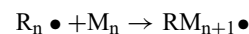
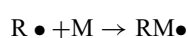
The first step of photopolymerization (or the creation of the "green part", that is to say the, non-post-treated sample) is almost always based on acrylate chemistry. Acrylates photopolymerize quickly and at ambient temperature, which makes them well adapted to 3D printing processes. Epoxy groups can also be added to generate Interpenetrated Polymer Networks (IPN). In IPN systems, acrylates initiate polymerization and the green part is subsequently heated to activate further epoxy polymerization.^[14,21] However, IPN systems will not be discussed in this review.

Acrylate monomers can polymerize due to their acrylate vinyl functional group, which undergoes a radical polymerization. In these reactions, the photoinitiator generates radical reactive species when excited at a specific wavelength in the UV spectrum. These reactive species initiate the polymerization of the monomers.^[21] As explained by Kim et al.^[38] three main steps can be distinguished in the photopolymerization reaction:

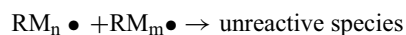
the initiation step:



the propagation steps:



and the termination:



where I refers to the photoinitiator that produces radicals (R•) under the action of UV light, M refers to the monomer, RM refers to a chain radical and RM_n refers to a polymer of n monomers. The vinyl double bond (C=C) is converted into a single bond during polymerization.^[38-40] This allows the determination of the degree of polymerization by quantifying the amount of double bonds that were converted. As a result, chemists use the term double bond conversion while physicists tend to speak of the degree of cure. The base acrylate resin can be modified by changing the photoinitiator concentration, its nature, or even by using different types of acrylate monomers. The resin formulation directly modifies the resin reactivity.

To compare and evaluate the different formulations and resin reactivity, P.F. Jacobs proposed a specific law in 1992 based on energetic considerations. Jacobs used the Beer-Lambert law to describe the exponential decrease of the light energy into the resin with the depth z:

$$E(z) = E_{\max} \exp(-z/D_p) \quad (1)$$

where D_p is the light penetration depth and E_{max} is the total light exposure dose at the resin surface. D_p is inversely proportional to the molar extinction coefficient of the initiator and its concentration. To pass the gel point, E(z) must reach the critical threshold energy E_c. This occurs when z=C_d (cure depth).

At this point:

$$E(C_d) = E_{\max} \exp(-C_d/D_p) = E_c \quad (2)$$

Finally, the commonly used Jacobs' law can be obtained from Eq. (2) and is written as follows^[41]:

$$C_d = D_p \ln \left(\frac{E_{\max}}{E_c} \right) \quad (3)$$

- C_d: Cure depth (μm)
- D_p: Light penetration depth in the resin (characteristic length) (μm).^[41]
- E_{max}: Exposure dose (mJ.cm⁻²); energy received at the resin surface during the curing.
- E_c: Critical exposure (mJ.cm⁻²); minimum amount of energy needed to start the curing process and reach the gel point.^[23,24,41-45]

Jacobs' law is applicable in the range D_p < C_d < 4D_p.^[41] The semi logarithmic plotting of C_d versus E_{max} is a straight line known as Jacobs' working curve [Fig. 1(d)]. One important point is that Jacobs' law gives information on intrinsic resin parameters (E_c and D_p) that do not depend on the printer or on experimental conditions.^[43] However, the control of the resin reactivity is necessary to adjust the printing parameters.

Historically, Jacobs' working curve applied for SLA printing. The laser scans particular areas of the liquid resin at

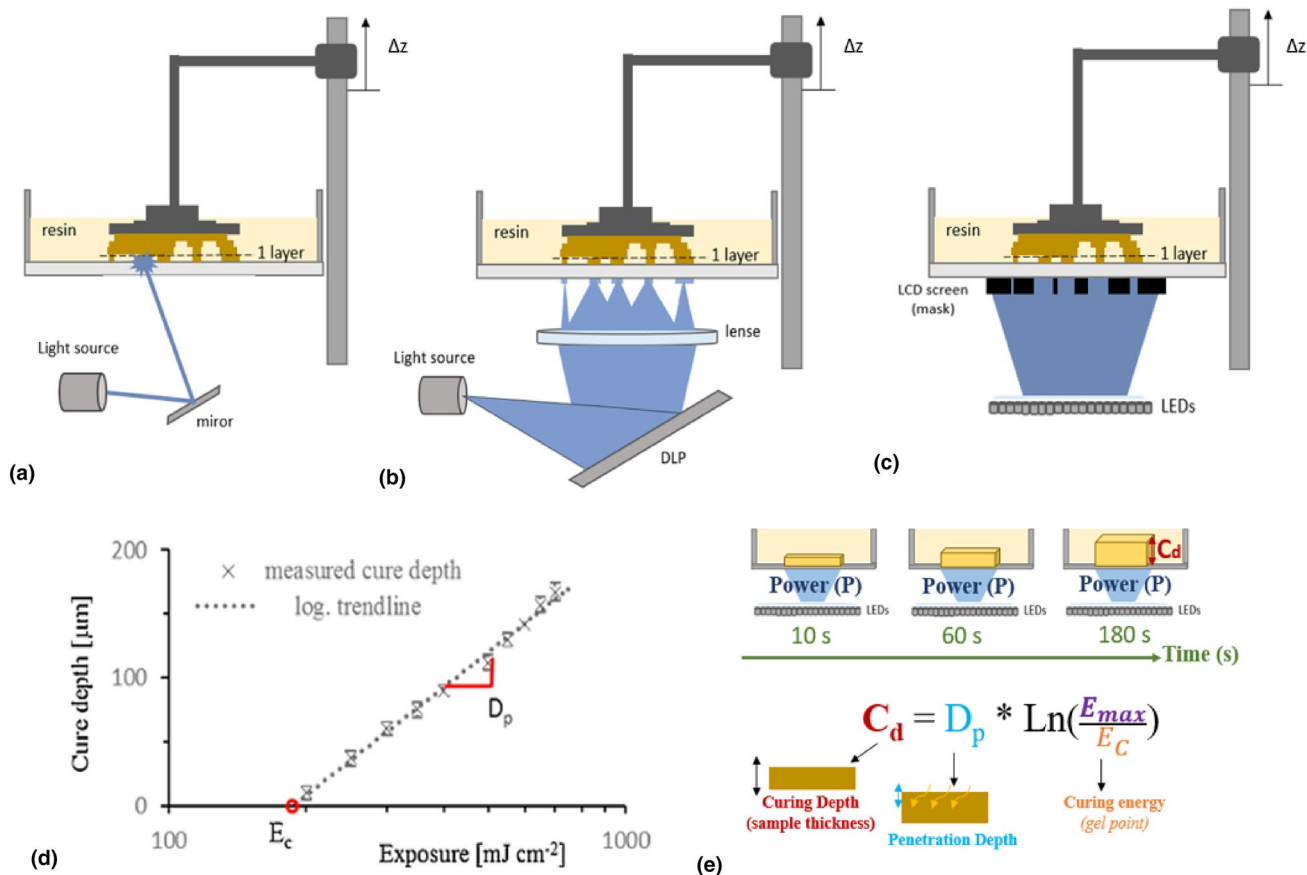


Figure 1. (a) Scheme of SLA apparatus. (b) DLP apparatus (c) LCD apparatus. (d) Example of a Jacobs' curve from Hofstetter et al. reproduced with authorization^[24] (e) Experimental methods to determine D_p and E_c for DLP or LCD printers.

different speeds. The higher the speed, the shorter the exposure to UV and therefore, the thinner the final object is. The height of the samples is directly measured with a caliper or a micrometer and corresponds to C_d .^[23] The exposure E_{max} is obtained with the following formula:

$$E_{max} = \frac{P_{laser}}{H_s V_s} \quad (4)$$

where P_{laser} is the laser power, H_s is the hatching (distance between laser scan lines) and V_s is the laser speed.^[23,41,44]

For DLP/LCD processes, D_p and E_c values are also obtained by exposing a pre-determined area with the same light power for different times, as illustrated in [Fig. 1(e)]. C_d (sample height) is also directly measured with a caliper or a micrometer, but in this case, E_{max} is obtained by multiplying the exposure time with the light power [Fig. 1(e)].^[40,46]

The large differences in reactivity between SLA, DLP and LCD resins are due to resin formulations which have been adapted to each process.^[24,41,47,48]

Thus, the reactivity of the resin is driven by its very composition, which directly influences the final mechanical properties of the printed part. For the rest of the study, we will focus on results obtained with DLP printing. A few LCD and SLA

studies are also treated, and we will precise for each case when LCD or SLA printing is concerned.

Influence of the resin composition on the mechanical properties Monomer nature and functionality

The first step of the formulation is the selection of monomers or a mixture of monomers and oligomers (Table II). As for all polymerization reactions, the choice of specific monomer (size, molecular weight, and chain rigidity when polymerized) directly affects the appearance of the printed object and its properties and, among them, its mechanical properties.

Several approaches can be found in the literature to confirm this direct relationship between the monomer structure and the final polymer properties. For example, Pooput et al. evaluated resin reactivity via Jacobs' curves and mechanical properties of their DLP-printed samples via tensile tests.^[49] They reported that formulations with flexible chains presented lower mechanical resistance (high strain and low tensile strength) whereas the formulations that contained rigid chains, with aromatics for example, were stiffer, due to the intrinsic structure of

chains. Similarly, Zhu et al. worked on healable and recyclable DLP-printed polymer and studied the mechanical properties of resins composed of two monoacrylates: urethane monoacrylate (UMA) and acrylic acid (AA) via tensile tests.^[27] They demonstrated that mechanical properties such as the Young's modulus, the tensile strength and the glass transition temperature could be tuned with different monomer ratios. Chen et al. also observed large changes in mechanical properties (e.g., Young's modulus and ultimate tensile strength) depending on the different monomer compositions and mixtures used.^[55] Indeed, increasing the proportion of harder oligomer increases the Young's modulus.

While commercial acrylate monomers are most commonly used, some authors chemically grafted acrylate groups to other types of monomers. For example, Field et al. modified a poly(caprolactone) with methacrylate groups. They carried out tensile tests and observed an increase of the Young's modulus from 0.7 to 4 MPa when the methacrylation substitution degree doubled from 40 to 80%.^[12] Chen et al. also observed a strong increase of Young's modulus (from 0.1 to 5.1 MPa) and of ultimate tensile strength when increasing the degree of acrylation from 7 to 30% with poly(glycerol sebacate) acrylate (PGSA) polymer printed with DLP.^[55]

The crosslinking density is also an important factor that influences mechanical properties. This crosslinking density is directly related to the number of acrylate groups in the monomer used, which is called functionality. For example, Miao et al. investigated the storage modulus of bio-based acrylate monomers with di- or tri-functionality (BHMP2 and BHMP3 respectively) printed via DLP method.^[56] The authors observed that the triacrylate presented a higher Young's modulus due to its compact and crosslinked structure. In the same way, Oezkan et al. worked on LCD and found that the curing performance increased with the amount of multifunctional oligomers in the formulation.^[48] Therefore, the cross-linker, which is a multifunctional acrylate, drives the network organization and thus the mechanical properties.

Dietz et al. studied the influence of the chain length and of pendant chains of di-, tri- and tetra-acrylate monomers. They mention that for linear di-functional monomers, the longer and softer the chain length, the higher the conversion degree.^[57] Concerning branched multifunctional monomers, the authors observed a decrease in the conversion degree for highly branched monomers. They explained that the branches cause steric hindrance, reducing the conversion degree.^[58] However, no mechanical characterization was performed.

Finally, Borrello et al. worked on DLP and demonstrated that according to the monomer/cross-linker ratio, a wide variety of Young's moduli can be obtained.^[25] They performed tensile tests and observed experimentally that a high quantity of 1,6-hexanediol diacrylate cross-linker (HDDA) strongly increased the Young's modulus. Additionally, the ultimate tensile strength was also slightly increased. Similarly, Shi et al.

studied the impact of different amounts of HDDA (di-acrylate) (Table II) on the mechanical properties via DMA studies.^[59] The authors observed an increase in the glass transition temperature, T_g , and an increase in the storage modulus as the proportion of HDDA monomer increased. They explained their observations by the fact that high HDDA content increases crosslinking in the polymer network. As a result, T_g increased due to the hampering of chain movement, and the stiffness (E) increased due to high chain crosslinking. Indeed, the authors showed by X-ray Diffraction (XRD) that the chains were more packed when the HDDA content increased.^[59] This might indicate the occurrence of more intense crosslinking due to the di-functional crosslinker (HDDA). This spatial arrangement generates a packing of the chains and consequently, an increase in stiffness.

These works demonstrate that the nature of the monomer and the proportion of different compounds influence the modulus, the ultimate tensile strength and the glass transition temperature.

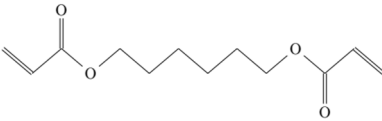
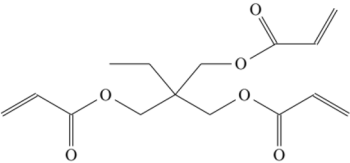
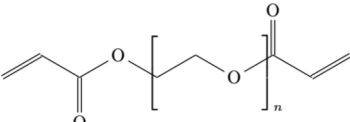
Photoinitiator

Another component of high importance for the photopolymerization reaction is the photoinitiator, which influences the photopolymerization kinetics and printing parameters (e.g., rheology, layer thickness, exposure time). In addition to that, its choice appears crucial to mechanical behavior.

For example Scherzer et al. demonstrated the different effects of three photoinitiators at the same concentration in an acrylate resin.^[60] They shed light on the different induction periods or conversion rates obtained depending on the nature of the photoinitiator.^[58,60,61] Moreover, not only the nature but also the concentration of the photoinitiator influences the printing parameters. Indeed, with a lower amount of photoinitiator, longer exposure times are needed to reach the same layer thickness.^[50] Gonzalez et al. observed very small variations in average viscosity when increasing the photoinitiator (BAPO) content in their formulations.^[50] However, Zanon et al., used camphorquinone as a photoinitiator and they observed different rheological behaviors depending on the camphorquinone content in their liquid resin (lower storage modulus with higher camphorquinone content, obtained by photo-rheology tests).^[62]

Additionally, several articles mention the existence of an optimum concentration of photoinitiator. Beyond this optimum, the further addition of photoinitiator does not improve the mechanical properties due to increased radical recombination. This shows a direct link between the photoinitiator content and mechanical properties.^[61,63,64] Wang et al. tried to optimize the concentration of the camphorquinone photoinitiator in their acrylate-based resin to achieve the best mechanical properties.^[65] They observed that the degree of conversion (obtained by near-infrared spectroscopy), the mechanical properties (elastic modulus and hardness), as well as the curing depth D_p (in Jacobs' law) were maximized for an optimum photoinitiator

Table II. Main components of a photopolymerization resin.

Resin component	Role and definition	Examples	Structures
Monomer	Contains one or several acrylate groups will generate a polymer composed of repetitive units	HDDA, TMPTA, PEGDA, UDMA, Bis-GMA ^[13]	
Oligomer	Small polymer (less than 10 repetitive units) containing one or several acrylate groups. Its longer chain increases the viscosity of the formulation	PEGDA (Mw=200, 500, 7000 g/mol), PEAAM ^[44]	1,6-hexanediol-diacrylate (HDDA)
Crosslinker	Monomer or oligomer that contain multifunctional acrylate and can crosslink monomers or oligomers densely	TMPTA or HDDA	
Photoinitiator	Chemical compound able to generate radical species when excited at a specific wavelength	Irgacure 819, ^[12] TPO, ^[49] BAPO, ^[50] DMPA ^[44]	Trimethylolpropane triacrylate (TMPTA)
Photoabsorber	Dye or photo-absorbing compound that consumes radical species and favors the termination process of polymerization	Sudan I, ^[51] III, Tinuvin ^[52]	
Plasticizer and Additives	Long soft polymer chains, often functionalized with acrylates that contributes to lowering the viscosity to favor printing	PEGDA, ^[53] TEGMA ^[54]	Poly(ethylene glycol) diacrylate (PEGDA)

concentration. This was also observed by Musanje et al. who shed light on the fact that the excess of photoinitiator (camphorquinone) could hamper the hardness.^[63] In the same way, Steyrer et al. found an optimal concentration by carrying out DMA and tensile tests to investigate the effect of three different photoinitiators.^[64]

As a result, these articles agree on the fact that the polymerization kinetics depends on the nature of the photoinitiator. In reviewing the literature, a concentration around 1–3 wt% of photoinitiator seems to be optimal in terms of mechanical properties.

Photoabsorber

With the increase of photoinitiator concentration, polymerization quickly initiates and there is a risk of an uncontrolled reaction. Such an uncontrolled propagation leads to a decrease in printing resolution. To avoid that, photoabsorbers are introduced in the system, in order to consume some of the radical species and, thus, to regulate the reaction propagation. Unlike photoinitiators that are consumed during the photopolymerization process, photoabsorbers remain active and undestroyed. Photoabsorbers are often dyes used to increase the printability and decrease D_p in Jacobs' law,^[12,24,52] but it is important to determine their effect on the final properties of the material.

Bagheri Saed et al. studied the influence of a photoabsorber (an orange dye) on the mechanical compression of their scaffold printed by DLP.^[66] They characterized their scaffold

with compressive tests for different exposures and different dye concentrations. The authors observed that the higher the light absorber content, the lower the compressive strength, whatever the exposure time [Fig. 2(a)]. They explained that a high amount of absorber hampers light penetration and thus decreases polymerization. The bonding between layers is weakened, which results in a lower compressive resistance. Hofstetter et al. presented a method to determine the best amount of photoabsorber.^[24] However, they did not evaluate the impact of the absorber on mechanical properties such as the Young's modulus.

As a result, photoabsorbers are mostly used to improve the printability and resolution of DLP/LCD printed objects, but tend to decrease the stiffness of materials. Nonetheless, few studies compare mechanical properties with and without photoabsorbers, and this is area deserves additional research.

Plasticizers and additives

Plasticizers decrease the viscosity of resins to ease the printing (Table II); they can also increase the resolution. However, they also have a negative impact on the mechanical properties.

For example, Yang et al. added a plasticizer (PEG300) to an acrylate formulation (based on PEGDA), and compared both the printability and mechanical properties via tensile tests.^[53] The authors observed an increase in strain and a decrease in ultimate tensile strength with the addition of a plasticizer [Fig. 2(b)]. Thus, if a small amount of plasticizer is helpful for

the printability, it also lowers the mechanical strength, and this must be considered in the design of the formulation.

Oezkan et al. investigated the effect of the content of HDDA as a diluent on the tensile properties of their LCD-printed objects.^[48] As the viscosity is a key parameter for the printability of resins, some diluents are added, such as TEGMA, to significantly increase printability.^[54] However, Lin et al. observed an increase in shrinkage with the diluent content.^[54] Shrinkage is the reduction of volume occupied by the resin during the polymerization process. Excessive shrinkage can cause the delamination of different printed layers. Furthermore, according to Yang et al. diluents like water can induce a decrease in hardness.^[53]

Thus, the use of plasticizers is interesting for highly viscous resins. However, improvements in the printability must be balanced against decreases in the Young's modulus due to plasticization.

Effect of printing parameters

Printing atmosphere: oxygen inhibition

As explained by Yamada and Goto: "Oxygen inhibition causes numerous undesirable effects on free radically cured products, including slow polymerization rate, long induction periods, low reaction conversion and tacky surface properties".^[68] Therefore, when it comes to acrylate photopolymerization, the consumption of radicals by oxygen can drastically influence the final material.

More precisely, an excess of oxygen leads to the incomplete polymerization of acrylate systems. Indeed, oxygen consumes the radicals and hinders the radical polymerization. Resulting materials are tacky and not completely polymerized [Fig. 2(c) under oxygen]. Even when the exposition time is increased, the problem persists.

On the other hand, a lack of oxygen leads to very strong and uncontrolled polymerization at the bottom of the vat. It can also lead to delamination between layers and difficulties in detaching the object. Deng et al. worked illustrated this in their DLP study by purging the resin of oxygen with argon, which led to uncontrolled curing due to total absence of inhibition [Fig. 2(c)]. To avoid these consequences, some solutions were found by manufacturers. Most often, the bottom of the vat is permeable to oxygen. This limits the polymerization of the part at the bottom of the vat. Thus, the force needed to lift-off the piece at the end of a layer printing is reduced. However, for LCD printers, where the vat is in direct contact with the screen, this solution is not applicable. Another possibility is the addition of a rake that mixes the resin between each layer. Finally, there is the tilt solution, which displaces the object laterally before uplifting the plate, limiting the suction forces.^[69,70]

As a result, the amount of oxygen in the resin must be controlled because it has direct consequences on the printability and on the interlayer adhesion. The presence of a dead zone or permanent liquid interface is favorable for good adhesion

between layers.^[71,72] Finally, the degree of oxygen inhibition is dependent of the resin formulation itself.^[73]

Curing temperature

The curing temperature is a very important parameter insofar as it directly influences the resin viscosity. The temperature is driven by the illumination system of the process (e.g., diode, laser, LED) and by the polymerization itself, which is exothermic. A few studies indicate that increasing the temperature can make printing easier and increase the conversion rate. However, the consequences on the mechanical properties are not well known.

According to Lu et al., using low temperatures might be interesting to reduce polymer shrinkage.^[74] Scherzer et al. compared an epoxy-acrylate and a trifunctional acrylate photopolymerization at different temperatures from ambient to 90°C.^[75] They observed an important increase in the acrylate conversion rate (obtained by real-time ATR-FTIR) with temperature.^[60] Sekmen et al. also made this observation in their DLP study.^[76] This result is attributed to a decrease in viscosity, which allows the faster diffusion of species in the medium.^[75] Moreover, the authors proved that increasing the temperature decreases the amount of dissolved oxygen in the resin. Therefore, a high curing temperature favors the initiation of the reaction. However, the authors did not link these results to mechanical properties. Steyrer et al. investigated the effect of curing temperature from 23 to 70°C for DLP photopolymerization of acrylate resins.^[39] They also concluded that the differences obtained were linked to the decrease in viscosity. The authors demonstrated the decrease of E_c in Jacobs' law when increasing the temperature: the polymerization could start at lower exposure.^[39]

As a result, increasing temperature permits not only a reduction in the printing time but also an increase in conversion rate. T_g is also increased, but the precise mechanisms are still not perfectly understood.^[38,77] The increase of the curing temperature might improve the mechanical properties such as the Young's modulus, but no clear demonstration has been made yet. More work is needed to confirm these trends and elucidate the mechanisms.

Exposure time

The exposure time and light power are of the utmost importance because they determine the conversion degree. Aznarte et al. observed a decrease of the elastic modulus with lower exposure times for DLP printed samples.^[78] The authors rationalized the result by the curing degree of the resin: lower curing time results in lower material stiffness, due to a lower conversion of acrylate groups.

On the contrary, for longer exposures, layers are exposed to a higher amount of light energy, thus, the conversion is higher and the interlayer zone is reinforced. This generates better adhesion between the layers and a higher Young's modulus (or stiffness). Bagheri Saed et al. also observed an increase in compressive strength with increasing exposure time for DLP.^[66] Similarly, Pyo et al. observed an increase in the stiffness of

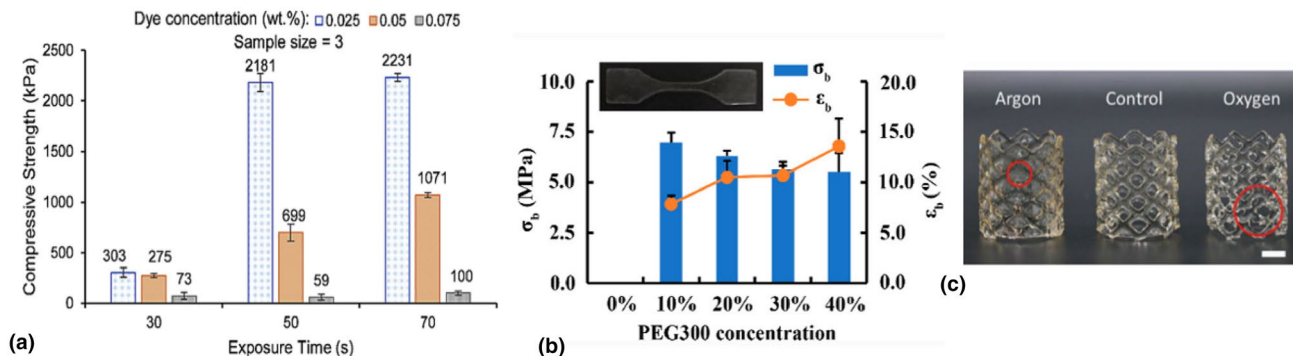


Figure 2. (a) Compressive strength of the scaffolds for different absorbers versus the exposure time, from Bagheri Saed et al. reproduced with authorization^[66] (b) Effect of a plasticizer (PEG300) on the mechanical properties, from Yang et al. reproduced with authorization^[53] (c) Results of the different structures printed in different atmospheres, from Deng et al. reproduced with authorization^[67]

their Digital micromirror device (DMD)-printed green chemistry-derived polyurethane with longer light exposures.^[79] Yang et al. investigated the effect of the exposure time of acrylate resin in DLP on the printability and the hardness.^[53] Concerning the mechanical properties, a strong increase in hardness was observed, which went from 0 to 107.2 N as the exposure was varied from 2 to 8 s. In the same way, Yao et al. generated microneedles for medical applications through DLP polymerization and evaluated the effect of exposure time on the mechanical performance in compression.^[80] They observed an increase in stiffness with the increase of exposure time, but a decrease in the resolution.

Thus, if the exposure time increases, the conversion degree and the stiffness increase, but the resolution decreases. High exposures also increase the force needed to raise the object from the vat, which might cause delamination issues. As a result, compromises must be achieved between accurate printing and good mechanical properties, insofar as an excess of exposure time leads to very long processes and over-cured scaffolds. It is also important to note that “dark polymerization” exists, and that the reaction continues even after turning off the UV light.^[22]

Layer thickness and sample size

Small layer thicknesses generate more cohesion and thus increase material stiffness. Indeed, Yang et al. mentioned that “reduced layer height was beneficial to printing accuracy but adverse to printing efficiency” due to the increase in printing time when using small layers.^[53] However, they did not study the consequences on mechanical properties. However, as mentioned by Keßler et al., small layer thicknesses increase the risk of printing error or void inclusion insofar as voids tend to appear in the interlayer area.^[81]

According to Kowalska, high layer thickness are detrimental because they increase polymer stress shrinkage during polymerization.^[15] This is in agreement with the results obtained by Wu et al. who observed higher distortion stress and higher bending curvatures for high layer height

samples.^[82] Nevertheless, anisotropy is reduced with higher layer thickness.

Concerning the sample size, most studies focus on the printer resolution, which reaches about 100 μm for the best performances.^[67,71] However, very few works focused on the size effect of bigger parts for DLP and LCD printing. Šťaffová et al. worked on DLP and studied the evolution of the network density obtained via DMA, depending on the sample thickness. They observed that “the deformation, glass transition temperature, molecular weight between entanglements and network density” were unchanged with the different sample thicknesses.^[40] However, no study observed the influence of the layer area on the mechanical properties.

Layer orientation

The layer-by-layer printing process generates anisotropy in the material and influences the stiffness as well as the fracture resistance. Steyrer et al. investigated the effect of orientation on the stiffness, measured by DMA and tensile testing for DLP printed samples.^[39] They observed that the green parts presented different behaviors depending on the printing direction. This was also observed by Keßler et al.^[81] Aznarte et al. observed that specimens printed by DLP in the Z direction (perpendicular to the tensile test direction) presented a lower tensile modulus and a lower ultimate tensile stress value^[78] [Fig. 3(a)]. This is due to the anisotropy generated by the process as well as the orientation of the tensile test itself. However, unexpectedly, the specimen printed in X and Y directions (both parallel to the tensile test direction) presented different moduli, stresses and strains, although there should be theoretically no difference (the layer is always printed in the XY plan). As a result, this might come from the printing parameters, an influence which is not fully understood yet. Thus, the orientation of layers during the printing process affects the Young’s modulus. Studies agree on the fact that higher moduli seem to be obtained when layers are oriented in the same direction as the tensile test.

This anisotropy is also observed in compression tests. For example, Wang et al. used DLP printing and demonstrated the existence of different behaviors of polyurethane acrylate resins in response to compression and tensile tests, depending on the orientation of the load.^[83] Indeed, they observed that compression of the samples led to less anisotropy.

On the contrary, in fracture studies, higher resistance is observed when the layers are perpendicular to the fracture stress. Štaffová et al. studied via DLP the effect of the orientation of the layer on the fracture resistance of samples [Fig. 3(b)].^[40] They observed important differences in the fracture resistance. With a stress applied in the Z direction, specimens printed with layers in the X direction presented the highest resistance to failure (layers perpendicular to the fracture stress) while samples with layers in the Z direction were less resistant. This might be due to weak interlayer bonding, which favors fracture propagation along the interlayer zone. The crack must go through every layer to break the whole material, which requires much more energy than the propagation along a weak interface [Fig. 3(c)]. Moreover, Keßler et al. observed by SEM microscopy fracture specimens printed by DLP in the Z direction and noted the presence of voids between two consecutive layers [Fig. 3(d)]. These voids might behave as weak points initiating fracture. The authors supposed these voids might be reduced by a better atmosphere and humidity control.^[84] Wang et al. analyzed the fracture morphology of the samples submitted to parallel and vertical tension as well as the crack formation of samples submitted to compression (both vertically and horizontally).^[83] The authors observed flatter tensile fracture morphology for samples submitted to vertical tension (perpendicular to the layers) while samples submitted to horizontal tension presented rougher crack surface. Thus, fracture resistance is highly anisotropic. However, fracture toughness is only defined for isotropic materials, i.e., materials that present the same properties in all directions. It is not the case here due to the anisotropy of the printing process (layer-by-layer). Wang et al. showed that the orientation has an influence on fracture resistance, but it might not be accurate enough to employ the term fracture toughness as defined by linear elastic fracture mechanics.

As a result, layer orientation drives the mechanical properties and the anisotropy of the final material. Process parameters are still not well understood and the differences in directions might come from the process itself. Furthermore, little attention is given to process defects like voids and inclusions that might induce interlayer weakness.

It is important to state that few studies include statistical analysis although many exploit the tensile test (Table III). This highly empirical method must be accompanied by statistical studies. In addition, repeatability studies concerning the printing are required to better understand the disparity and defects of the printed materials.

Other printing parameters

As showed in the review by Al Rashid et al. dedicated to composites, the main parameters investigated for increasing the Young's modulus, tensile strength, flexural strength, hardness and compressive strength have been the layer thickness, the exposure time, the concentration of acrylate oligomer and the light intensity.^[86] However, other printing parameters remain unexplored such as the effect of the retracting speed. Indeed, after the printing of each layer, the plate on which the object is fixed goes up to allow the printing of the next layer. To our current knowledge, the speed at which the plate moves is not studied in the literature although it generates a lot of stress on the resin. Its local viscosity might be changed depending on the applied speed, which might result in different layer thicknesses for different rising speeds. Additionally, printing parameters such as the local heating of the screen and the pixel resolution are rarely studied. Zinelis et al. printed the same resin with different 3D printers (LCD and DLP) and observed significant dispersions in some mechanical measurements (hardness and indentation modulus for example).^[85] This emphasizes the importance of device-specific parameters.

As a result, the printing parameters are still not completely mastered due to their high number and the intrinsic correlations between them. This is also because they are not always accessible to users. The exploration of the various printing parameters is intrinsically made difficult by the printers themselves because not all parameters can be modified. As presented in Table III, many parameters have been investigated, but the corresponding chemical characterization is often missing to fully understand the changes at the molecular or mesoscopic scale. Additionally, another processing step: the post-treatment, also strongly determines the mechanical properties.

Effect of post-processing

Layer-by-layer printing generates a raw printed object called the "green part". This green part is always subjected to post-treatments including washing steps and insolation with UV light to achieve total polymer conversion^[87] (Table IV).

Washing steps

Printing is followed by a washing step (mostly with isopropanol for acrylates) to eliminate the residual uncured monomers from the object surface. This washing step seems to influence the mechanical performance; to some extent, it depends on the solvent. This was observed by Bardelcik et al., who printed polymethyl methacrylate (PMMA) resin with SLA. They observed variations in Young's modulus with the solvents used (e.g., isopropanol, detergent, hydrogen peroxide).^[88] They observed an increase of the strain of the samples loaded via tensile test due to the plasticization induced by the solvent washing. Jang et al. investigated the effect of washing conditions on the flexural strength and conversion degree of objects printed by DLP.^[89] No significant difference in surface roughness for the different

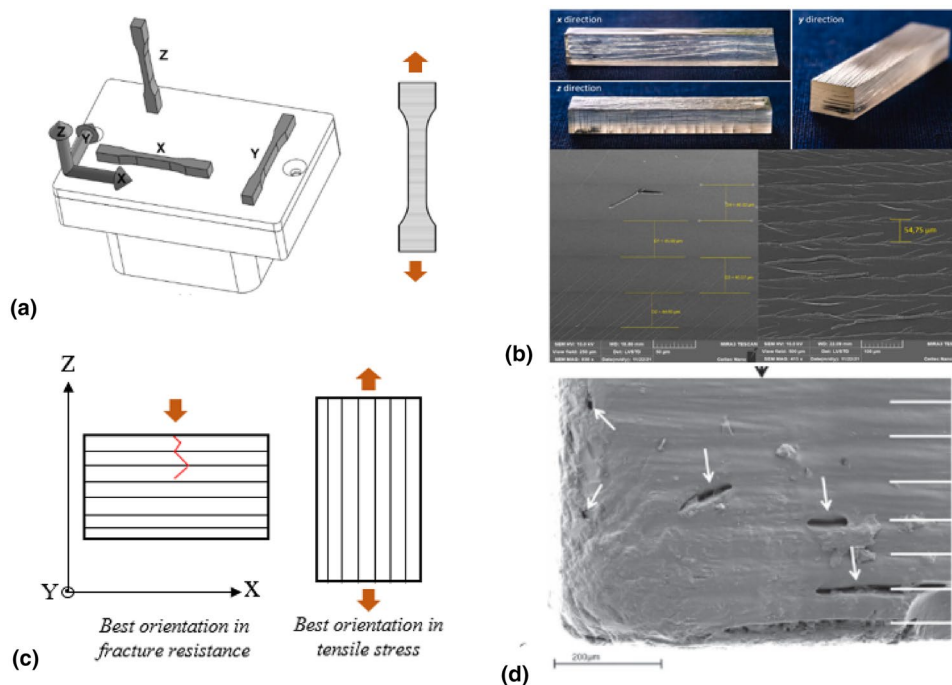


Figure 3. (a) Scheme of the 3 orientations tested in tensile test Aznarte et al., reproduced with authorization^[78] (b) samples printed in X, Y and Z direction and SEM images of these samples, taken from Štaffová et al. reproduced with authorization^[40] (c) Scheme of the best orientations to optimize fracture resistance or Young's modulus, (d) SEM picture of horizontal parallel printing and fracture initiation at the surface of voids, arrows indicate the propagation, which was initiated at the void positions, by Keßler et al. reproduced with authorization^[81]

conditions was observed, whereas a significant difference in conversion degrees was obtained (via FTIR measurements). The authors explained that inefficient washings might result in over-curing during post-treatment while highly washed samples present suspended solid particles that could be responsible for the roughness. In the same way, Lambart et al. investigated the flexural strength in three point bending tests of dental acrylate-based resins printed in DLP submitted to different washing treatments and report similar observations.^[90]

Concerning fracture resistance, Hargreaves mentioned the ability of solvents like ethanol or soap solutions to initiate cracks in PMMA with more damage than water.^[93] Indeed, according to Štaffová et al., isopropanol washing can lead to the initiation of cracks in their DLP printed material.^[40]

As a result, the washing steps generate swelling and weaken the inter-layer zones, decreasing the ultimate tensile strength and Young's modulus (Table IV). There is still a lack of knowledge on the washing of DLP and LCD printed objects: what is the best washing protocol for each resin? Is it preferable to use one long wash or several shorter washes per sample?

Post-curing

Post-curing consists of insulating and exposing to UV-light the freshly printed samples, also called green parts. During this crucial step, the polymerization continues, redefining the mechanical properties. However, the amount of light received,

the post-curing temperature, the post-curing duration and even the post-curing methods, drastically affects the final properties (Table IV).

Štaffová et al. observed via SEM analysis that a 30-min post-treatment with UV further polymerized the interlayer zones [Fig. 3(b)].^[40] The post-treatment resulted in an increase in failure temperature, T_g and storage modulus obtained via DMA measurements. Similarly, Steyrer et al. observed that the Young's modulus and tensile strength of the green samples were significantly increased after the post-treatment.^[39] The increase of modulus after UV post-treatment is due to the densification of the polymer network as observed by an increase in the material rigidity. The increase of post-treatment time increases the network density and T_g in the same way, tending to an asymptotic limit. Thus, UV post-treatment increases the Young's modulus, double bond conversion, and T_g .

But a major problem with post-curing, whatever the 3D printing method, is the distortion of the objects, as described by Wu et al.^[82] The authors analyzed the shape of the samples during UV exposure (post-treatment) with a camera to estimate the curvature. They tried to link it to the post-treatment process and other printing parameters. They observed a UV-induced bending (a final distortion) amplified for low thicknesses.^[41] Nevertheless, uncertainties and disagreements remain concerning the post-curing kinetics. Besides, one legitimate question

Table III. Outline of experimental works linking printing parameters to mechanical properties.

Main idea	Type of printer	Resin chemistry	PI content	Jacobs law parameters	Printing parameters investigated	Chemical analysis	Mechanical properties	Mechanical tests	Microscopy?	Main conclusion
Scherzer et al. ^[60] There is a temperature dependence on the solubility of oxygen in acrylate resin	No printer	Tripropylene glycol diacrylate (TPGDA) and bisphenol A epoxy diacrylate—photoinitiators Irgacure 819 Darocur 1173	1 wt%	N.I	Atmosphere/oxygen inhibition	Real-time ATR-FTIR, UV-visible	N.I	N.I	N.I	The induction period decreases with temperature (due to lower Oxygen solubility)
Deng et al. ^[67] Rapid printing of thermoplastic polymer is possible when controlling 2 competing processes: polymerization and polymer dissolution	DLP	ACMO (4-acryloylmorpholine) monomer, Sudan III as photosensitizer, Irgacure 819 as photoinitiator	N.M	N.I	Atmosphere/oxygen inhibition	FTIR- Melt and dissolution tests	Young modulus	Tensile test	N.I	Absence of oxygen leads to uncontrolled curing while too high oxygen content leads to low printability accuracy
Scherzer et al. ^[75] Understand how temperature influences the photopolymerization kinetics of diacrylate	No printer	Tripropylene glycol diacrylate (TPGDA) and a bisphenol A epoxy diacrylate oligomer (BA-EpAc), different photoinitiators investigated	0.1 and 1 wt%	N.I	Curing temperature	Real-time ATR-FTIR, viscosity, DSC, GA	N.I	N.I	N.I	A high curing temperature favors the initiation of the reaction and the degree of conversion, mostly due to the viscosity reduction

Table III. (continued)

	Main idea	Type of printer	Resin chemistry	PI content	Jacobs law parameters	Printing parameters investigated	Chemical analysis	Mechanical properties	Mechanical tests	Microscopy?	Main conclusion
Steyer et al. ^[39]	Hot VS room temperature printing of a dimethyl acrylate	DLP	Bisphenol-A-dimethyl acrylate-based resin, BAPO photoinitiator and light absorber UV-1995 (photoabsorber)	N.M	$E_c \approx 10 \text{ mJ/cm}^2$ and $D_p \approx 70\text{--}80 \text{ }\mu\text{m}$	Curing temperature/layer orientation	Rheometer, ATR-FTIR spectroscopy	T _g , E, tensile stress	DMA	SEM observations	Increasing the temperature decreases Ec. Lower mechanical properties for layers oriented in the Z direction (anisotropy)
Štaffová et al. ^[40]	Improvement of printing, post-printing and thermomechanical properties of photopolymerization resins	DLP	Commercial acrylate transparent clear resin, TPO photoinitiator	6 wt%	$E_c = 3,3\text{--}5,7 \text{ mJ/cm}^2$ and $D_p = 187 \text{ to } 360 \text{ }\mu\text{m}$	Post-curing/layer orientation	HDT, photo-DSC,	T _g , E, rubber modulus, strain, hardness, network density	DMA	SEM observations	Post-curing time and print orientation affect mechanical properties. Possible uncured regions in the layer boundary
Chan Kim et al. ^[38]	Uv-curing kinetics and performance of curable materials	Multi-Jet	Commercial UV-curable 3D printing resin (Vero WhitePlus RGD 835), photoinitiator, diphenyl-2,4,6-trimethylbenzoyl phosphine oxide	2 wt%	N.I	Curing temperature	ATR-FTIR (for conversion rate)	T _g	Differential scanning calorimetry (DPC) and DSC	N.I	Possible description of the T _g depending on UV curing. Increased curing temperature increases the conversion degree

Table III. (continued)

Main idea	Type of printer	Resin chemistry	PI content	Jacobs law parameters	Printing parameters investigated	Chemical analysis	Mechanical properties	Mechanical tests	Microscopy?	Main conclusion
Yang et al. ^[53] Printability of DLP structures: Influence of a plasticizer on the printability and mechanical properties	DLP	PEGDA, PEG300 as a plasticizer, DPPO as a photoinitiator, tartrazine, methylene blue and cococine as photoabsorbers	1 wt%	N.I	Exposure time/layer thickness	N.I	Young modulus, stress, strain, hardness	Tensile test, compression test, hardness test	N.I	Decreasing layer height increases printing accuracy. Increasing exposure time increases hardness
Pyo et al. ^[79] 3D printing of green aliphatic polyurethanes	DMD	Diurethanes functionalized with methacrylate, photoinitiator lithium phenyl-2,4,6-trimethylbenzoylphosphinate (LAP)	2% (w/v)	N.I	Exposure time	FT-IR, UV-visible, DSC	N.I	N.I	N.I	Increase of material stiffness with the increase of exposure time
Aznarte et al. ^[78] Anisotropic tensile consideration of DLP printed materials	DLP	Commercial standard clear resin (PR-48)	N.M	N.I	Exposure time/layer thickness/ orientation	N.I	Elastic modulus, ultimate stress, ultimate strain	Tensile test (n=6)	N.I	Small layer thickness and long exposure times increase elastic modulus, and ultimate stress. Higher mechanical properties in the X/Y direction

Table III. (continued)

Main idea	Type of printer	Resin chemistry	PI content	Jacobs law parameters	Printing parameters investigated	Chemical analysis	Mechanical properties	Mechanical tests	Microscopy?	Main conclusion
Thermomechanical properties of stereolithography printed parts	SLA	Formlabs clear resin	N.M	N.I	Layer thickness/printing orientation	ATR-FTIR (for conversion rate)	T _g , E	DMA	Optical microscopy	Decreasing layer thickness increases T _g . No significant difference in parallel or perpendicular orientation for SLA
Mechanics of shape distortion of DLP structures during post-curing—modelling	DLP	PEGDA, Irgacure 819 and Sudan I as photoabsorber	0,69 wt%	N.I	Layer thickness	ATR-FTIR (for conversion rate)	N.I	N.I	N.I	Higher stress and higher bending curvatures for high layer thickness samples
Influence of printing direction on the flexural strength and modulus of 3D-printed materials	DLP	Methacrylate based commercial dental resins	1–5 wt%	N.I	Layer orientation	N.I	Flexural strength and flexural modulus, Weibull parameters	Three-point bending tests	SEM observations	Higher mechanical properties in the X direction: layers play the role of "crack arrester". Voids in the interlayer zone are weak points inducing fracture

Table III. (continued)

Main idea	Type of printer	Resin chemistry	PI content	Jacobs law parameters	Printing parameters investigated	Chemical analysis	Mechanical properties	Mechanical tests	Microscopy?	Main conclusion
Yong-Hong et al. ^[77] Mechanicals properties of curable resins	PolyJet	Acrylic monomer/Isobornyl acrylate/ Phenol, 4,4'-(1-methylethyldiene) bis-, polymer with (chloromethyl) oxirane, 2-propenoate/Diphenyl-2,4,6-trimethylbenzoyl phosphine oxide	N.M	N.I	Layer orientation	DSC, DPC	T _g , Elastic modulus, ultimate stress, ultimate strain, tensile toughness	Tensile test (n=8)	Optical microscopy	"The anisotropic properties are clearly seen in tensile toughness and elongation at break with respect to a printing direction, while it is not seen in their Young's modulus and tensile strength" for this PolyJet study
Zinelis et al. ^[85] Comparative analysis of different 3D printers resulting mechanical properties	DLP and LCD	Commercial resin used in dentistry (Tera Harz TC- 85DAW, Graphy, Seoul, Korea)	N.M	N.I	Difference between LCD and DLP	N.I	Martens-Hardness, indentation-modulus and elastic-index	Hardness testing machine	N.I	Different mechanical properties due to different irradiance conditions but also to parameters such as the resolution or the layer thickness

NI not investigated, *MM* not mentioned.

Table IV. Outline of experimental works linking post-treatment parameters to mechanical properties.

Ref	Main idea	Type of printer	Washing treatment	Post-curing method	Mechanical properties	Mechanical tests	Main conclusion
Štaffová et al. ^[40]	Improvement of printing, post-printing and thermomechanical properties of photopolymerization resins	DLP	Isopropanol for less than 15 s	Prusa CW1 curing 10 mW cm ⁻² at 35 °C	E, Tg, G'	DMA, HDT, tensile test	Isopropanol washing increases defects, delamination and swelling. Post-curing
Bardelcik et al. ^[88]	Influence of washing treatment on mechanical properties of 3D printed PMMA	DLP	Isopropyl Alcohol (IP) (60 and 90%), Hydrogen Peroxide (HP) (2,5 and 5%), Detergent (D)—10 min at ambient temperature	N.I	E, tensile strength, tensile strain (at break)	Tensile test	Washing treatments consequences depend on the solvent nature. Risk of swelling and increase in strain with prolonged washings
Jang et al. ^[89]	Effect of the washing treatment on the fracture strength and the conversion degree	DLP	Isopropyl alcohol (IPA) for 5 s, 1 min or 10 min, tripropylene glycol monomethyl ether (TPM) for 10 min	N.I	Roughness, contact angle, flexural strength	Optical profiler, contact angle device, three-point flexural fracture test	The degree of conversion increased with the increase of washing time. Residual monomers do not affect flexural strength in a significant way
Lambart et al. ^[90]	Effect of the washing treatment on the roughness and flexural strength	DLP	IPA, ethanol (EtOH), EASY 3D Cleaner (EYC), Yellow Magic7 (YM7), and RESINAWAY (RAY)	Light-curing unit (Otofash G171) with 2 × 2000 flashes (λ from 280 to 700 nm) under a nitrogen atmosphere	Roughness, flexural strength	Three point bending test	Flexural strength significant differences depending on the solvent. No significant difference in roughness
Zguris et al. ^[91]	Influence of UV-curing on mechanical properties of stereolithography parts	SLA	N.I	UV light at 365, 385 and 405 nm at 25 °C, 44 °C and 60 °C	Young modulus, ultimate tensile strength	Tensile test	Reaching full post-curing increases the Young modulus and tensile strength (high temperature and long exposures) at the best wavelength
Mendes Felipe et al. ^[92]	Evaluation of post-curing process on the thermomechanical properties of SLA resin	SLA	2-propanol in two successive 15 min baths	Post-curing without any source of light and with the exposure to an UV light at 371 nm wavelength and 2.0–2.5 mWcm ⁻² for 5 min, 30 min, and 2, 5, 15, 20, 24 and 30 h	Tg, E', E''	DSC, TGA, DMTA (Dynamic mechanical thermal analysis)	Complete cure achieved in 30 h without and with UV-light. Post-curing process influences curing degree and thus mechanical properties

Table IV. (continued)

Ref	Main idea	Type of printer	Washing treatment	Post-curing method	Mechanical properties	Mechanical tests	Main conclusion
Yong-Hong et al. ^[77]	Mechanicals properties of curable resins	PolyJet	N.M	UV and electron beam are compared	Tg, Tensile strength, Young's modulus, elongation at break, isotropy	DSC, DPC, tensile test	Electron beam treatment increases mechanical properties and erases the size dependent and anisotropic behaviors
Keßler et al. ^[81]	Influence of printing direction on the flexural strength and modulus of 3D-printed materials	DLP	Rinsing with 96% ethanol	Postcured for 2 × 2,000 flashes under a nitrogen atmosphere and thermocycling aging for some samples	Flexural strength and flexural modulus, Weibull parameters	Three-point bending tests	Thermocycling aging decreases failure probability (Weibull plots)
Wu et al. ^[82]	Mechanics of shape distortion of DLP structures during post-curing—modeling	DLP	N.M	UV post-curing for different times	curvature / distortion	modelization of curvature	Distortion results in z degree of conversion gradient generated during the postcuring
Salmoria et al. ^[87]	Evaluation of post-curing stereolithography parameters	SLA	N.M	1 h in a UV chamber (300 W), or 4 min in a Toshiba microwave oven (700 W), or under isothermal treatment at 125 °C for 30 min in a conventional oven	Tg, shrinkage, shore hardness	Dilatometer, DSC, hardness machine	Defects appear in the structure due to uncured resin trapped in the cured network. Thermal post-cured leads to better performances
Steyrer et al. ^[39]	Hot VS room temperature printing of a dimethacrylate	DLP	N.M	UV flood curing for 2 × 300 s at 100% intensity	Tg, E, tensile strength	DMA	The UV post-curing leads to similar properties even if the two materials were not cured at the same temperature

Table V. Final table of the consequences of resin and printing parameters on mechanical properties.

Parameter	Mechanical consequences	Reference
Increase the ratio of rigid monomer/oligomer	Modulus increase by a factor 8, Tensile strength increase by a factor 5, Hardness increase by a factor 3 (for the specific formulations compared) Possible increase of Young's modulus by a factor 3	Pooput et al. ^[49] Chen et al. ^[55]
Addition of an acrylate cross-linker	Increase of T_g (of 50°C) Can increase the Young's modulus from 1 to 30 MPa Can increase the T_g up to 56%	Zhu et al. ^[27] Borrello et al. ^[25] Shi et al. ^[59]
Increase of the methacrylation degree	Increase of the Young's modulus from 0,7 to 4 MPa when the methacrylation degree doubled from 40 to 80%	Field et al. ^[12]
Increase of functionality (from -di, to -tri acrylates)	Tensile strength increase of 20 MPa and Young's modulus increase by a factor 5 (for the specific di and tri acrylate used)	Miao et al. ^[56]
Photoinitiator	Existence of an optimum amount of photoinitiator that maximizes flexural modulus and Young's modulus (photoinitiator dependent) Existence of an optimum amount of photoinitiator that maximizes hardness	Lima et al. ^[61] Musanje et al. ^[63]
Photoabsorber	Nature and concentration of photoinitiator influences yield strength. Maximum yield strength obtained for 1.18 wt % TPO-L Decrease in compression strength (2.2 MPa to 0.1 MPa with a dye concentration from 0.025 to 0.075 wt%)	Steyrer et al. ^[64] Bagheri Saed et al. ^[66]
Plasticizers	Decrease in tensile strength from 7.0 to 5.5 MPa as PEG300 content increased from 10 to 40%	Yang et al. ^[53]
Printing atmosphere	Mostly studies on the resin reactivity—lack of mechanical characterizations	Scherzer et al. ^[60]
Printing T°C	Increase of Young's modulus and T_g with high curing temperature (70°C instead of 20°C)	Steyrer et al. ^[39]
Layer thickness	Small layers increase Young's modulus (increase layers from 10 to 50 μm decreased Young's modulus from 1000 to 600 MPa) Small layers increase Young's modulus (increase layers from 50 to 200 μm decreased Young's modulus from 900 to 300 MPa)	Park et al. ^[26] Aznarte et al. ^[78]
Layer orientation	X direction presents higher failure resistance (when stress perpendicular to layers) Z direction presents lower Young's modulus and tensile strength (when stress perpendicular to layers)	Štaffová et al. ^[40] Aznarte et al. ^[78]
Washing step	Decrease of Young's modulus (from 800 MPa to about 500 MPa and 400 MPa for some solvent) Decrease of flexural strength for some solvent	Bardelcik et al. ^[88] Lambart et al. ^[90]
UV Post-treatment	Increase of Young's modulus, tensile strength (factor 2) and T_g with post-treatment	Steyrer et al. ^[39]

concerns the post-treatment of porous and cellular materials of precise architecture: which one should be chosen? Should it be adapted to the density? Is there a gradient of polymerization from the surface to the core of post-treated objects?

As explained by Jang et al., research concerning the influence of the post-treatment is very scarce whereas numerous studies focus on improving the printing resolution.^[89] However, the post-treatment drives the mechanical properties (Table IV) and should be further studied especially with DLP/LCD technology.

Summary and perspectives

This review revealed the numerous challenges in DLP and LCD 3D printing. While literature is still scarce for LCD printing, DLP studies reveal that this new process is quite complex,

with many distinct parameters (summarized Table V). From a chemistry viewpoint, the components of the resin control both the reactivity and the final properties such as the stiffness. The amount and nature of photoinitiator or monomer used can drastically change the resin properties, and thus the properties of the printed material. Besides, not only the resin but also the numerous parameters (atmosphere, temperature, exposure time, layer thickness and orientation...) of the layer-by-layer printing have to be considered. Indeed, they strongly influence both printability and the final mechanical stiffness. Finally, the post-treatment plays an important role in the determination of final mechanical properties and should be further studied.

Therefore, while many advances in understanding the links between the resin materials and the final mechanical properties of 3D printed objects have been achieved, many questions

remain unsolved. New models and parameters might be necessary to better understand the processes.^[46] Concerning the chemistry of the resin, the liquid state is often well-described, but more research needs to be done concerning the final green part. More mechanical and thermomechanical analysis should be performed to evaluate the influence of the photoabsorber on mechanical properties and interlayer cohesion. Furthermore, statistical analysis should be employed more systematically in these different studies. Indeed, uncertainties are multiplied not only by the characterization techniques themselves, but also by the printing, which has not been proven to be absolutely repeatable. Additionally, the role of defects, and more precisely at the interlayer zone, must be studied further. Besides, these 3D printing processes generate intrinsic residual stress, mostly due to shrinkage of the final materials.^[41,94] Further work is needed first to characterize and quantify this mechanical residual stress and then to control and reduce it via heat post-treatments, for example. More generally, increased knowledge of the different printing parameters is needed and could allow the conception of new devices and optimized processes.

Acknowledgments

The authors thank Mark Levenstein for his help in writing the paper.

Funding

This work is supported by a public grant overseen by the French National Research Agency (ANR) as part of the “Investissements d’Avenir” program (Labex NanoSaclay, reference: ANR-10-LABX-0035 and Labex PALM, reference: ANR-10-LABX-0039-PALM). This work was also funded by ESILV, CEA, CEA PTC Materials program and CEA Focus circular economy program.

Open Access

This article is licensed under a Creative Commons Attribution 4.0 International License, which permits use, sharing, adaptation, distribution and reproduction in any medium or format, as long as you give appropriate credit to the original author(s) and the source, provide a link to the Creative Commons licence, and indicate if changes were made. The images or other third party material in this article are included in the article’s Creative Commons licence, unless indicated otherwise in a credit line to the material. If material is not included in the article’s Creative Commons licence and your intended use is not permitted by statutory regulation or exceeds the permitted use, you will need to obtain permission directly from the copyright holder. To view a copy of this licence, visit <http://creativecommons.org/licenses/by/4.0/>.

References

1. C.K. Hull, Apparatus for production of three-dimensional objects by stereolithography. Google Patents **1986**, US4575330B1 (1986)
2. M. Pagac et al., A review of vat photopolymerization technology: Materials, applications, challenges, and future trends of 3d printing. *Polymers (Basel)* **13**(4), 1–20 (2021). <https://doi.org/10.3390/polym13040598>
3. J. Huang, Q. Qin, J. Wang, A review of stereolithography: processes and systems. *Processes* (2020). <https://doi.org/10.3390/PR8091138>
4. A. Su and S. J. Al’Aref (2018) Chapter 1 History of 3D Printing. In: S. J. Al’Aref, B. Mosadegh, S. Dunham, and J. K. Min (Eds). *3D Printing Applications in Cardiovascular Medicine*, Elsevier, USA
5. K.D. Jandt, R.W. Mills, A brief history of LED photopolymerization. *Dent. Mater.* **29**(6), 605–617 (2013). <https://doi.org/10.1016/j.dental.2013.02.003>
6. Z. Weng, Y. Zhou, W. Lin, T. Senthil, L. Wu, Structure-property relationship of nano enhanced stereolithography resin for desktop SLA 3D printer. *Compos. Part A Appl. Sci. Manuf.* **88**, 234–242 (2016). <https://doi.org/10.1016/j.compositesa.2016.05.035>
7. J.Z. Manapat, Q. Chen, P. Ye, R. C. Advincula, 3D printing of polymer nanocomposites via stereolithography. *Macromol. Mater. Eng.* **302**(9), 1–13 (2017). <https://doi.org/10.1002/mame.201600553>
8. S.A. Rasaki, D. Xiong, S. Xiong, F. Su, M. Idrees, Z. Chen, Photopolymerization-based additive manufacturing of ceramics: a systematic review. *J. Adv. Ceram.* **10**(3), 442–471 (2021). <https://doi.org/10.1007/s40145-021-0468-z>
9. R. Palucci Rosa, G. Rosace, Nanomaterials for 3D printing of polymers via stereolithography: concept, technologies, and applications. *Macromol. Mater. Eng.* **306**(10), 1–19 (2021). <https://doi.org/10.1002/mame.20210345>
10. J. Zhang, Q. Hu, S. Wang, J. Tao, M. Gou, Digital light processing based three-dimensional printing for medical applications. *Int. J. Bioprinting* **6**(1), 12–27 (2020). <https://doi.org/10.18063/ijb.v6i1.242>
11. N.A. Chartrain, C.B. Williams, A.R. Whittington, A review on fabricating tissue scaffolds using vat photopolymerization. *Acta Biomater.* **74**, 90–111 (2018). <https://doi.org/10.1016/j.actbio.2018.05.010>
12. J. Field, J.W. Haycock, F.M. Boissonade, F. Claeysens, A tuneable, photocurable, poly(caprolactone)-based resin for tissue engineering—synthesis, characterisation and use in stereolithography. *Molecules* (2021). <https://doi.org/10.3390/molecules26051199>
13. A. Bagheri, J. Jin, Photopolymerization in 3D printing. *ACS Appl. Polym. Mater.* **1**(4), 593–611 (2019). <https://doi.org/10.1021/acsapm.8b00165>
14. S.C. Ligon, R. Liska, J. Stampfl, M. Gurr, R. Mülhaupt, Polymers for 3D printing and customized additive manufacturing. *Chem. Rev.* **117**(15), 10212–10290 (2017). <https://doi.org/10.1021/acs.chemrev.7b00074>
15. A. Kowalska, J. Sokolowski, K. Bociong, The photoinitiators used in resin based dental composite—a review and future perspectives. *Polymers (Basel)* **13**(3), 1–17 (2021). <https://doi.org/10.3390/polym13030470>
16. F. Kotz et al., Three-dimensional printing of transparent fused silica glass. *Nature* **544**(7650), 337–339 (2017). <https://doi.org/10.1038/nature22061>
17. M.S. Pham, C. Liu, I. Todd, J. Lerthanasarn, Damage-tolerant architected materials inspired by crystal microstructure. *Nature* **565**(7739), 305–311 (2019). <https://doi.org/10.1038/s41586-018-0850-3>
18. Q. Ge et al., Projection micro stereolithography based 3D printing and its applications. *Int. J. Extrem. Manuf.* (2020). <https://doi.org/10.1088/2631-7990/ab8d9a>
19. N.A. Traugutt, D. Mistry, C. Luo, K. Yu, Q. Ge, C.M. Yakacki, Liquid-crystal-elastomer-based dissipative structures by digital light processing 3D printing. *Adv. Mater.* **32**(28), 1–7 (2020). <https://doi.org/10.1002/adma.202000797>
20. S.H. Park, M. Kaur, D. Yun, W.S. Kim, Hierarchically designed electron paths in 3D printed energy storage devices. *Langmuir* **34**(37), 10897–10904 (2018). <https://doi.org/10.1021/acs.langmuir.8b02404>
21. C. Decker, Photoinitiated crosslinking polymerisation. *Prog. Polym. Sci.* **21**, 593–650 (1996)
22. C. Decker, K. Moussa, A new method for monitoring ultra-fast photopolymerizations by real-time infra-red (RTIR) spectroscopy. *Die Makromol.*

- Chemie **189**(10), 2381–2394 (1988). <https://doi.org/10.1002/macp.1988.021891016>
23. M. Invernizzi, R. Suriano, A. Muscatello, S. Turri, M. Levi, Near-visible stereolithography of a low shrinkage cationic/free-radical photopolymer blend and its nanocomposite. *J. Appl. Polym. Sci.* (2020). <https://doi.org/10.1002/app.48333>
 24. C. Hofstetter, S. Orman, S. Baudis, J. Stampfl, Combining cure depth and cure degree, a new way to fully characterize novel photopolymers. *Addit. Manuf.* **24**, 166–172 (2018). <https://doi.org/10.1016/j.addma.2018.09.025>
 25. J. Borrello, P. Nasser, J.C. Iatridis, K.D. Costa, 3D printing a mechanically-tunable acrylate resin on a commercial DLP-SLA printer. *Addit. Manuf.* **23**, 374–380 (2018). <https://doi.org/10.1016/j.addma.2018.08.019>
 26. S. Park, A.M. Smallwood, C.Y. Ryu, Mechanical and thermal properties of 3d-printed thermosets by stereolithography. *J. Photopolym. Sci. Technol.* **32**(2), 227–232 (2019). <https://doi.org/10.2494/photopolymer.32.227>
 27. G. Zhu, Y. Hou, J. Xiang, J. Xu, N. Zhao, Digital light processing 3D printing of healable and recyclable polymers with tailorable mechanical properties. *ACS Appl. Mater. Interfaces* **13**(29), 34954–34961 (2021). <https://doi.org/10.1021/acscami.1c08872>
 28. O. Konuray, J.M. Morancho, X. Fernández-Francos, M. García-Alvarez, X. Ramis, Curing kinetics of dually-processed acrylate-epoxy 3D printing resins. *Thermochim. Acta* (2021). <https://doi.org/10.1016/j.tca.2021.178963>
 29. J.L. Halary, F. Laupretre, L. Monnerie, *Polymer materials: macroscopic properties and molecular interpretations* (Wiley, 2011)
 30. F. Zhang et al., The recent development of vat photopolymerization: a review. *Addit. Manuf.* (2021). <https://doi.org/10.1016/j.addma.2021.102423>
 31. H. Quan, T. Zhang, H. Xu, S. Luo, J. Nie, X. Zhu, Photo-curing 3D printing technique and its challenges. *Bioact. Mater.* **5**(1), 110–115 (2020). <https://doi.org/10.1016/j.bioactmat.2019.12.003>
 32. W. Piedra-Cascón, V.R. Krishnamurthy, W. Att, M. Revilla-León, 3D printing parameters, supporting structures, slicing, and post-processing procedures of vat-polymerization additive manufacturing technologies: a narrative review. *J. Dent.* (2021). <https://doi.org/10.1016/j.jdent.2021.103630>
 33. D. Ahn, L.M. Stevens, K. Zhou, Z.A. Page, Rapid high-resolution visible light 3D printing. *ACS Cent. Sci.* **6**(9), 1555–1563 (2020). <https://doi.org/10.1021/acscentsci.0c00929>
 34. P. Fiedor, J. Ortyl, A new approach to micromachining: high-precision and innovative additive manufacturing solutions based on photopolymerization technology. *Materials* (Basel) **13**(13), 1–25 (2020). <https://doi.org/10.3390/ma13132951>
 35. H. Goodarzi Hosseinabadi, E. Dogan, A.K. Miri, L. Ionov, Digital light processing bioprinting advances for microtissue models. *ACS Biomater. Sci. Eng.* **8**(4), 1381–1395 (2022). <https://doi.org/10.1021/acsbomaterials.1c01509>
 36. M.G.A. Mohamed, H. Kumar, Z. Wang, N. Martin, B. Mills, K. Kim, Rapid and inexpensive fabrication of multi-depth microfluidic device using high-resolution LCD stereolithographic 3D printing. *J. Manuf. Mater. Process.* **3**(1), 1–11 (2019). <https://doi.org/10.3390/jmmp3010026>
 37. W. Shan, Y. Chen, M. Hu, S. Qin, P. Liu, 4D printing of shape memory polymer via liquid crystal display (LCD) stereolithographic 3D printing. *Mater. Res. Express* (2020). <https://doi.org/10.1088/2053-1591/abd05>
 38. Y.C. Kim et al., UV-curing kinetics and performance development of in situ curable 3D printing materials. *Eur. Polym. J.* **93**, 140–147 (2017). <https://doi.org/10.1016/j.eurpolymj.2017.05.041>
 39. B. Steyrer, B. Busetti, G. Harakály, R. Liska, J. Stampfl, Hot Lithography vs. room temperature DLP 3D-printing of a dimethacrylate. *Addit. Manuf.* **21**, 209–214 (2018). <https://doi.org/10.1016/j.addma.2018.03.013>
 40. M. Štaffová, F. Ondraáš, J. Svatík, M. Zbončák, J. Jančář, P. Lepcio, 3D printing and post-curing optimization of photopolymerized structures: Basic concepts and effective tools for improved thermomechanical properties. *Polym. Test.* (2022). <https://doi.org/10.1016/j.polymertesting.2022.107499>
 41. P.F. Jacobs, Rapid prototyping & manufacturing—fundamentals of stereolithography. *J. Manuf. Syst.* **12**(5), 430–433 (1993). [https://doi.org/10.1016/0278-6125\(93\)90311-g](https://doi.org/10.1016/0278-6125(93)90311-g)
 42. Y. Li et al., Isotropic stereolithography resin toughened by core-shell particles. *Chem. Eng. J.* **394**, 124873 (2020). <https://doi.org/10.1016/j.cej.2020.124873>
 43. S. Zakeri, M. Vippola, E. Levänen, A comprehensive review of the photopolymerization of ceramic resins used in stereolithography. *Addit. Manuf.* **35**, 101177 (2020). <https://doi.org/10.1016/j.addma.2020.101177>
 44. T. Chartier, A. Badev, Y. Aboulatim, P. Lebaudy, L. Lecamp, Stereolithography process: Influence of the rheology of silica suspensions and of the medium on polymerization kinetics—Cured depth and width. *J. Eur. Ceram. Soc.* **32**(8), 1625–1634 (2012). <https://doi.org/10.1016/j.jeurceramsoc.2012.01.010>
 45. C.J. Bae, J.W. Halloran, Integrally cored ceramic mold fabricated by ceramic stereolithography. *Int. J. Appl. Ceram. Technol.* **8**(6), 1255–1262 (2011). <https://doi.org/10.1111/j.1744-7402.2010.02568.x>
 46. J. Lee et al., Average-accumulated normalized dose (A-AND) predicts ultimate tensile strength and elastic modulus of photopolymer printed by vat photopolymerization. *Addit. Manuf.* (2022). <https://doi.org/10.1016/j.addma.2022.102799>
 47. Y. Li, Q. Mao, J. Yin, Y. Wang, J. Fu, Y. Huang, Theoretical prediction and experimental validation of the digital light processing (DLP) working curve for photocurable materials. *Addit. Manuf.* (2021). <https://doi.org/10.1016/j.addma.2020.101716>
 48. B. Oezkan, F. Sameni, S. Karmel, D.S. Engström, E. Sabet, A systematic study of vat-polymerization binders with potential use in the ceramic suspension 3D printing. *Addit. Manuf.* (2021). <https://doi.org/10.1016/j.addma.2021.102225>
 49. K. Pooput, S. Channasanon, P. Tesavibul, P. Pittayavinai, W. Taweelue, Photocurable elastomers with tunable mechanical properties for 3D digital light processing printing. *J. Polym. Res.* **27**(10), 1–10 (2020). <https://doi.org/10.1007/s10965-020-02289-w>
 50. G. González et al., Materials testing for the development of biocompatible devices through vat-polymerization 3d printing. *Nanomaterials* **10**(9), 1–13 (2020). <https://doi.org/10.3390/nano10091788>
 51. X. Kuang, Z. Zhao, K. Chen, D. Fang, G. Kang, H.J. Qi, High-speed 3D printing of high-performance thermosetting polymers via two-stage curing. *Macromol. Rapid Commun.* **39**(7), 1–8 (2018). <https://doi.org/10.1002/marc.201700809>
 52. R. Bail, J.Y. Hong, B.D. Chin, Effect of a red-shifted benzotriazole UV absorber on curing depth and kinetics in visible light initiated photopolymer resins for 3D printing. *J. Ind. Eng. Chem.* **38**, 141–145 (2016). <https://doi.org/10.1016/j.jiec.2016.04.017>
 53. Y. Yang, Y. Zhou, X. Lin, Q. Yang, G. Yang, Printability of external and internal structures based on digital light processing 3D printing technique. *Pharmaceutics* **12**(3), 1–16 (2020). <https://doi.org/10.3390/pharmaceutics12030207>
 54. C.H. Lin, Y.M. Lin, Y.L. Lai, S.Y. Lee, Mechanical properties, accuracy, and cytotoxicity of UV-polymerized 3D printing resins composed of Bis-EMA, UDMA, and TEGDMA. *J. Prosthet. Dent.* **123**(2), 349–354 (2020). <https://doi.org/10.1016/j.prosdent.2019.05.002>
 55. J.Y. Chen et al., Study of physical and degradation properties of 3D-printed biodegradable, photocurable copolymers, PGSA-co-PEGDA and PGSA-co-PCLDA. *Polymers* (Basel) (2018). <https://doi.org/10.3390/polym10111263>
 56. J.T. Miao et al., Three-dimensional printing fully biobased heat-resistant photoactive acrylates from aliphatic biomass. *ACS Sustain. Chem. Eng.* **8**(25), 9415–9424 (2020). <https://doi.org/10.1021/acssuschemeng.0c02168>
 57. J.E. Dietz, N.A. Peppas, Reaction kinetics and chemical changes during polymerization of multifunctional (meth)acrylates for the production of highly crosslinked polymers used in information storage systems. *Polymer* (Guildf) **38**(15), 3767–3781 (1997). [https://doi.org/10.1016/s0032-3861\(96\)00902-0](https://doi.org/10.1016/s0032-3861(96)00902-0)
 58. E. Andrzejewska, Photopolymerization kinetics of multifunctional monomers. *Prog. Polym. Sci.* **26**(4), 605–665 (2001). [https://doi.org/10.1016/S0079-6700\(01\)00004-1](https://doi.org/10.1016/S0079-6700(01)00004-1)
 59. Y. Shi et al., Chapter 8—Materials for four-dimensional printing (section 8.3.4—Acrylate-based shape memory polymer), in *3D printing technology series, materials for additive manufacturing*. ed. by Y. Shi, C. Yan, Y. Zhou, Y.W. Wu, S. Yu, Y. Chen (Academic Press, 2021), pp.679–739

60. T. Scherzer, H. Langguth, Temperature dependence of the oxygen solubility in acrylates and its effect on the induction period in UV photopolymerization. *Macromol. Chem. Phys.* **206**(2), 240–245 (2005). <https://doi.org/10.1002/macp.200400300>
61. C. Dos Reis Lima, D.B. da Silva, R.P. Vitti, M.E. Miranda, W.C. Brandt, Mechanical properties of experimental resin cements containing different photoinitiators and co-initiators. *Clin. Cosmet. Investig. Dent.* **11**, 285–290 (2019). <https://doi.org/10.2147/CCIDE.S221742>
62. M. Zanon, D. Baruffaldi, M. Sangermano, C.F. Pirri, F. Frascella, A. Chiappone, Visible light-induced crosslinking of unmodified gelatin with PEGDA for DLP-3D printable hydrogels. *Eur. Polym. J.* (2021). <https://doi.org/10.1016/j.eurpolymj.2021.110813>
63. L. Musanje, J.L. Ferracane, R.L. Sakaguchi, Determination of the optimal photoinitiator concentration in dental composites based on essential material properties. *Dent. Mater.* **25**(8), 994–1000 (2009). <https://doi.org/10.1016/j.dental.2009.02.010>
64. B. Steyrer, P. Neubauer, R. Liska, J. Stampfl, Visible light photoinitiator for 3D-printing of tough methacrylate resins. *Materials (Basel)* **10**(12), 1–11 (2017). <https://doi.org/10.3390/ma10121445>
65. K. Wang, B. Li, K. Ni, Z. Wang, Optimal photoinitiator concentration for light-cured dental resins. *Polym. Test.* (2021). <https://doi.org/10.1016/j.polymertesting.2020.107039>
66. A. Bagheri Saed, A.H. Behraves, S. Hasannia, S.A. Alavinasab Ardebili, B. Akhouni, M. Pourghayoumi, Functionalized poly L-lactic acid synthesis and optimization of process parameters for 3D printing of porous scaffolds via digital light processing (DLP) method. *J. Manuf. Process.* **56**, 550–561 (2020). <https://doi.org/10.1016/j.jmapro.2020.04.076>
67. S. Deng, J. Wu, M.D. Dickey, Q. Zhao, T. Xie, Rapid open-air digital light 3D printing of thermoplastic polymer. *Adv. Mater.* (2019). <https://doi.org/10.1002/adma.201903970>
68. S. Yamada, Y. Goto, Reduction of oxygen inhibition in photopolymerization of cyclic allylic sulfide monomer. *J. Photopolym. Sci. Technol.* **23**(1), 109–114 (2010). <https://doi.org/10.2494/photopolymer.23.109>
69. H. He, J. Xu, X. Yu, Y. Pan, Effect of constrained surface texturing on separation force in projection stereolithography. *J. Manuf. Sci. Eng. Trans. ASME* **140**(9), 1–9 (2018). <https://doi.org/10.1115/1.4040322>
70. X. Wu, Q. Lian, D. Li, Z. Jin, Tilting separation analysis of bottom-up mask projection stereolithography based on cohesive zone model. *J. Mater. Process. Technol.* **243**, 184–196 (2017). <https://doi.org/10.1016/j.jmatpotech.2016.12.016>
71. J.R. Tumbleston et al., Continuous liquid interface production of 3D objects. *Science* **347**(6228), 1349–1352 (2015). <https://doi.org/10.1126/science.aaa2397>
72. M.P. De Beer, H.L. Van Der Laan, M.A. Cole, R.J. Whelan, M.A. Burns, T.F. Scott, Rapid, continuous additive manufacturing by volumetric polymerization inhibition patterning. *Sci. Adv.* (2019). <https://doi.org/10.1126/sciadv.aau8723>
73. T.Y. Lee, C.A. Guymon, E.S. Jönsson, C.E. Hoyle, The effect of monomer structure on oxygen inhibition of (meth)acrylates photopolymerization. *Polymer (Guildf)* **45**(18), 6155–6162 (2004). <https://doi.org/10.1016/j.polymer.2004.06.060>
74. B. Lu, P. Xiao, M. Sun, J. Nie, Reducing volume shrinkage by low-temperature photopolymerization. *J. Appl. Polym. Sci.* **104**, 1126–1130 (2006). <https://doi.org/10.1002/app.25758>
75. T. Scherzer, U. Decker, The effect of temperature on the kinetics of diacrylate photopolymerizations studied by real-time FTIR spectroscopy. *Polymer (Guildf)* **41**(21), 7681–7690 (2000). [https://doi.org/10.1016/S0032-3861\(00\)00141-5](https://doi.org/10.1016/S0032-3861(00)00141-5)
76. K. Sekmen, T. Rehbein, M. Johlitz, A. Lion, A. Constantinescu, Thermal analysis and shrinkage characterization of the photopolymers for DLP additive manufacturing processes. *Contin. Mech. Thermodyn.* (2022). <https://doi.org/10.1007/s00161-022-01137-0>
77. S.Y. Hong et al., Experimental investigation of mechanical properties of UV-Curable 3D printing materials. *Polymer (Guildf)* **145**, 88–94 (2018). <https://doi.org/10.1016/j.polymer.2018.04.067>
78. E. Aznarte, C. Ayranci, A.J. Qureshi, Digital light processing (DLP): anisotropic tensile considerations, in *Proceedings of the 28th Annual International Solid Freeform Fabrication Symposium*, Austin, TX, USA, 7–9 August 2017, pp. 413–425
79. S.H. Pyo, P. Wang, H.H. Hwang, W. Zhu, J. Warner, S. Chen, Continuous optical 3D printing of green aliphatic polyurethanes. *ACS Appl. Mater. Interfaces* **9**(1), 836–844 (2017). <https://doi.org/10.1021/acsami.6b12500>
80. W. Yao et al., 3D Printed multi-functional hydrogel microneedles based on high-precision digital light processing. *Micromachines* (2020). <https://doi.org/10.3390/mi11010017>
81. A. Keßler, R. Hickel, N. Ilie, In vitro investigation of the influence of printing direction on the flexural strength, flexural modulus and fractographic analysis of 3d-printed temporary materials. *Dent. Mater. J.* **40**(3), 641–649 (2021). <https://doi.org/10.4012/dmj.2020-147>
82. D. Wu, Z. Zhao, Q. Zhang, H.J. Qi, D. Fang, Mechanics of shape distortion of DLP 3D printed structures during UV post-curing. *Soft Matter* **15**(30), 6151–6159 (2019). <https://doi.org/10.1039/c9sm00725c>
83. Y. Wang, X. Li, Y. Chen, C. Zhang, Strain rate dependent mechanical properties of 3D printed polymer materials using the DLP technique. *Addit. Manuf.* **47**, 102368 (2021). <https://doi.org/10.1016/j.addma.2021.102368>
84. S.C. Ligon, B. Husár, H. Wutzler, R. Holman, R. Liska, Strategies to reduce oxygen inhibition in photoinduced polymerization. *Chem. Rev.* **114**(1), 577–589 (2014). <https://doi.org/10.1021/cr3005197>
85. S. Zinelis, N. Panayi, G. Polychronis, S.N. Papageorgiou, T. Eliades, Comparative analysis of mechanical properties of orthodontic aligners produced by different contemporary 3D printers. *Orthod. Craniofac. Res.* **5**(3), 1–6 (2021). <https://doi.org/10.1111/ocr.12537>
86. A. Al Rashid, W. Ahmed, M.Y. Khalid, M. Koç, Vat photopolymerization of polymers and polymer composites: processes and applications. *Addit. Manuf.* **47**, 102279 (2021). <https://doi.org/10.1016/j.addma.2021.102279>
87. G.V. Salmoria, C.H. Ahrens, V.E. Beal, A.T.N. Pires, V. Soldi, Evaluation of post-curing and laser manufacturing parameters on the properties of SOMOS 7110 photosensitive resin used in stereolithography. *Mater. Des.* **30**(3), 758–763 (2009). <https://doi.org/10.1016/j.matdes.2008.05.016>
88. A. Bardelcik, S. Yang, F. Alderson, A. Gadsden, The effect of wash treatment on the mechanical properties and energy absorption potential of a 3D printed polymethyl methacrylate (PMMA). *Mater. Today Commun.* (2021). <https://doi.org/10.1016/j.mtcomm.2020.101728>
89. W. Jang et al., Effect of washing condition on the fracture strength, and the degree of conversion of 3d printing resin. *Appl. Sci.* **11**(24), 3–11 (2021). <https://doi.org/10.3390/app112411676>
90. A.-L. Lambart, A.B. Xepapadeas, B. Koos, P. Li, S. Spintzyk, Rinsing post-processing procedure of a 3D-printed orthodontic appliance material: impact of alternative post-rinsing solutions on the roughness, flexural strength and cytotoxicity. *Dent. Mater.* **366**, 1–10 (2022). <https://doi.org/10.1016/j.dental.2022.06.010>
91. Z. Zguris, *How mechanical properties of stereolithography 3D prints are affected by UV curing* (Formalabs Inc., Somerville, 2017)
92. C. Mendes-Felipe, D. Patrocínio, J.M. Laza, L. Ruiz-Rubio, J.L. Vilas-Vilela, Evaluation of postcuring process on the thermal and mechanical properties of the Clear02™ resin used in stereolithography. *Polym. Test.* **72**(October), 115–121 (2018). <https://doi.org/10.1016/j.polymertesting.2018.10.018>
93. A.S. Hargreaves, The effect of the environment on the crack initiation toughness of dental poly(methyl methacrylate). *J. Biomed. Mater. Res.* **15**(5), 757–768 (1981). <https://doi.org/10.1002/jbm.820150511>
94. D. Xie, F. Lv, Y. Yang, L. Shen, Z. Tian, A review on distortion and residual stress in additive manufacturing. *Chin. J. Mech. Eng. Addit. Manuf. Front.* (2022). <https://doi.org/10.1016/j.cjmeam.2022.100039>

Publisher's Note Springer Nature remains neutral with regard to jurisdictional claims in published maps and institutional affiliations.